Cancer Research

Ovarian Cancer Chemoresistance Relies on the Stem Cell Reprogramming Factor PBX1

Jin-Gyoung Jung[1], Ie-Ming Shih[1,2,3], Joon Tae Park[1], Emily Gerry[1], Tae Hoen Kim[1], Ayse Ayhan[1,4,5], Karen Handschuh[6], Ben Davidson[7,8], Amanda N. Fader[1,2,3], Licia Selleri[6], and Tian-Li Wang[1,2,3]

Abstract

The evolution of chemoresistance is a fundamental characteristic of cancer that ultimately hampers its clinical management. However, it may be possible to improve patient outcomes significantly by a better understanding of resistance mechanisms, which cancers rely upon during the evolution to an untreatable state. Here we report an essential role of the stem cell reprogramming factor, PBX1, in mediating chemoresistance in ovarian carcinomas. In the clinical setting, high levels of PBX1 expression correlated with shorter survival in post-chemotherapy ovarian cancer patients. In tumor cells with low endogenous levels of PBX1, its enforced expression promoted cancer stem cell-like phenotypes, including most notably an increase in resistance to platinum-based therapy used most commonly for treating this disease. Conversely, silencing PBX1 in platinum-resistant cells that overexpressed PBX1 sensitized them to platinum treatment and reduced their stem-like properties. An analysis of published genome-wide chromatin immunoprecipitation data indicated that PBX1 binds directly to promoters of genes involved in stem cell maintenance and the response to tissue injury. We confirmed direct regulation of one of these genes, STAT3, demonstrating that the PBX1 binding motif at its promoter acted to positively regulate STAT3 transcription. We further demonstrated that a STAT3/JAK2 inhibitor could potently sensitize platinum-resistant cells to carboplatin and suppress their growth *in vivo*. Our findings offer a mechanistic rationale to target the PBX1/STAT3 axis to antagonize a key mechanism of chemoresistance in ovarian cancers and possibly other human cancers. *Cancer Res; 76(21); 6351–61. ©2016 AACR.*

Introduction

Cytoreductive surgery followed by cycles of platinum/taxane chemotherapy has become the standard treatment for advanced epithelial ovarian cancer. Although most ovarian tumors initially respond to chemotherapy, refractory tumors often emerge as a result of clonal expansion of either acquired or innately resistant tumor cells, which ultimately develop into recurrent tumors. Consequently, up to 80% of women with advanced stage ovarian high-grade serous carcinoma (HGSC) experience recurrence after first-line chemotherapy, and the 5-year survival rate is only approximately 40% in these patients (1).

Several theories have been proposed to explain the development of chemoresistance in human cancer. A prevailing view is that heterogeneous cell subpopulations, which exhibit different degrees of tumor-initiating potentials and drug sensitivities, exist within a tumor. Alternatively, cancer cells may acquire these phenotypes during tumor evolution in the presence of selective pressures such as cytotoxic agents and hypoxia. The dynamic interplay between tumor cells and their microenvironment may activate developmental pathways, such as Wnt and Notch, that allow them to survive and expand. Reactivation of developmental pathways equips tumor cells with "stemness," which is characterized by self-renewal, repopulation, and resistance to cytotoxic insult (2). Therefore, it is critical to identify genes and pathways involved in this process to further understand the molecular underpinnings of stem cell–like cancer cells (CSC) and their relation to the bulk population of tumor cells (3). This new knowledge would guide the design of more effective cancer therapeutic strategies.

In this study, we collected primary and matched recurrent/chemoresistant tumor tissues from 41 patients with ovarian HGSC and analyzed the expression levels of stem cell factors. We found that the homeodomain transcription factor PBX1 is significantly upregulated in recurrent ovarian tumors. Functional studies demonstrated that PBX1 expression is essential for promoting platinum resistance. In addition, we delineated PBX1-regulated transcriptional networks that may account for its involvement in the development of drug resistance and stemness.

[1]Department of Pathology, Johns Hopkins Medical Institutions, Baltimore, Maryland. [2]Department of Oncology, Johns Hopkins Medical Institutions, Baltimore, Maryland. [3]Department of Gynecology and Obstetrics, Johns Hopkins Medical Institutions, Baltimore, Maryland. [4]Department of Pathology, Seirei Mikatahara Hospital, Hamamatsu, Japan. [5]Department of Pathology, Hamamatsu University School of Medicine, Hamamatsu, Japan. [6]Department of Cell and Developmental Biology, Weill Medical College, Cornell University, New York, New York. [7]Department of Pathology, Oslo University Hospital, Norwegian Radium Hospital, Oslo, Norway. [8]Faculty of Medicine, Institute of Clinical Medicine, University of Oslo, Oslo, Norway.

Note: Supplementary data for this article are available at Cancer Research Online (http://cancerres.aacrjournals.org/).

Current address for L. Selleri: Program in Craniofacial Biology, Departments of Orofacial Sciences & Anatomy, University of California, San Francisco, San Francisco, California.

Corresponding Author: Tian-Li Wang, Johns Hopkins Medical Institutions, CRBII, Room 306, 1550 Orleans Street, Baltimore, MD 21231. Phone: 410-502-0863; E-mail: tlw@jhmi.edu

doi: 10.1158/0008-5472.CAN-16-0980

Materials and Methods

Tumor specimens and cell lines

Tissue microarrays containing 41 pairs of matched primary and recurrent tumor tissues were constructed using deidentified samples from HGSC patients who underwent optimal surgical debulking at the Johns Hopkins Hospital (Baltimore, MD). Another cohort consisted of ascites tumor samples from patients who had undergone optimal debulking surgery at the Norwegian Radium Hospital. Institutional review board approval was obtained for each study cohort.

Human ovarian cancer cell lines, including OVCAR3, SKOV3, and Hey, were purchased from the ATCC during year 2006—8. IOSE-80PC, a cell line derived from normal ovarian surface epithelium, was a kind gift from Dr. Nelly Auersperg (University of British Columbia, British Columbia, Canada). MPSC1, a low-grade ovarian serous carcinoma cell line, was previously described (4). To establish chemoresistant ovarian cancer cells, SKOV3, OVCAR3, and MPSC1 cells were cultured for 3–6 months in the continuous presence of 10 μmol/L carboplatin (Sigma-Aldrich). Primary and carboplatin-resistant cell lines as well as IOSE-80PC were authenticated by genetic profiling using eight polymorphic short tandem repeat (STR) loci plus amelogenin in year 2015–2016.

Mouse fallopian tube epithelium (mFTE) was cultured by scraping the tubal mucosal surface from *Pbx1*$^{fl/fl}$ mice (5, 6). To establish immortalized cell lines, primary cultures were infected with the Simian virus 40 large T antigen (SV40 LTag), and single clones were isolated. The epithelial origin of immortalized cell lines was confirmed by positivity for EpCAM or cytokeratin 8 protein markers. The Müllerian origin was supported by the expression of PAX8 protein. Cells were incubated with Ade-Cre (1×10^7 pfu) or with Ade-GFP for 12 hours. The deletion of the Pbx1 allele and the loss of Pbx1 protein were assessed by Western blot analysis as detailed in the Supplementary Methods.

Analyses of cancer stem cell phenotypes

To identify the side population, we incubated cells with Hoechst 33342 (5 μg/mL), either alone or in the presence of 50 μg/mL verapamil. Cell suspension was then analyzed on an LSRII flow cytometer (Becton Dickinson). Hoechst 33342 dye was excited with a UV laser at 350 nm, and its fluorescence emission was measured with 405 nm/BP309 (Hoechst blue) and 570/BP20 (Hoechst red) optical filters.

Cells positive for aldehyde dehydrogenase (ALDH) activity were identified by staining with the ALDEFLUOR reagent (Stemcell Technologies). An aliquot of cells was treated with 5 μL of 1.5 mmol/L diethylaminobenzaldehyde (DEAB), a specific ALDH inhibitor, and served as a negative control. Cells were analyzed on an LSRII flow cytometer using the FL1 channel. Data were analyzed using CELLQuest Pro (BD Biosciences).

A hanging-drop culture method was performed to facilitate the generation of multicellular spheroids (7). Briefly, 1,000 suspension cells were dispensed into each well of a Gravity TRAP plate (Insphero) in 10% FBS culture medium and incubated for 24 hours. Cell clusters were then seeded in ultralow attachment plates (Corning), and the sphere size was measured by width and length every 3 days for 12 days.

Drug sensitivity assay

All chemicals, including carboplatin, paclitaxel, and methotrexate, were purchased from Sigma. Cells were seeded in 96-well plates at a density of 3,000 cells per well in triplicate and treated with serial dilutions of chemotherapeutic drugs. Cell viability was measured after 72 hours with CellTiter-Blue reagent (Promega) using a microplate reader (Fluostar, BMG). The data are presented as mean ± SD, calculated from triplicate values, and IC_{50} was defined as the concentration that resulted in a 50% decrease in the number of live cells. For the colony formation assay, 1,000 cells were seeded into a 35-mm culture dish. After 9 days, the cells were stained with crystal violet dye (Sigma-Aldrich).

Luciferase reporter assay

Human *STAT3* promoter regions of various lengths were amplified and cloned into the pGL3-basic plasmid. Microdeletion of the PBX1 consensus binding motif on the *STAT3* promoter was generated using a Site-Directed Mutagenesis Kit (Agilent). 293FT cells were then transfected with either PBX1 or pcDNA6 and cotransfected with various STAT3 promoter constructs. pRL-*Renilla* reporter plasmid (Promega) was cotransfected for assessing transfection efficiency. Luciferase activity was determined by the Dual-Luciferase reporter assay system (Promega); firefly luciferase activity was normalized to *Renilla* luciferase activity.

In vitro dual-color competition assay

PBX1-negative cells were transiently transfected with either pcDNA6-PBX1-V5 or pcDNA6. CellTracker Red CMTPX Dye (Molecular Probes) was used to label pcDNA6-transfected cells following the manufacturer's instructions. PBX1-positive and PBX1-negative cells were mixed at a 1:1 ratio and cocultured in a medium containing 0, 25, or 50 μmol/L of carboplatin for 6 days. Cells were then briefly fixed using 4% paraformaldehyde in PBS, incubated with anti-V5-FITC antibody to stain for PBX1-V5–positive cells, and visualized by fluorescence microscopy (Nikon, TE-200). Cells were plated in triplicate wells. PBX1-positive and PBX1-negative cells were visually counted in five high power fields containing at least 100 cells per field. The ratio of green FITC-stained (PBX1-positive) cells to red CMTPX-stained (PBX1-negative) cells was determined.

Chromatin immunoprecipitation and electrophoretic mobility shift assay

Chromatin immunoprecipitation (ChIP) was performed as described previously (8). Electrophoretic mobility shift assay (EMSA) was performed using the methods previously described by us (9–11). Both methods were detailed in the Supplementary Methods.

Xenograft of chemoresistant ovarian cancer

All animal procedures were approved by the Johns Hopkins Animal Care and Use Committee (protocol number: M012M405 and M015M127). SKOV3^{CR} or OVCAR8^{CR} cells (3×10^6 each) were injected subcutaneously into 6-week-old athymic nude mice. When palpable tumors developed, mice were randomized into four treatment groups ($n = 7$ for each group): group 1 was treated with vehicle control; group 2 was treated with ruxolitinib alone (10 mg/kg body weight); group 3 was treated with carboplatin alone (30 mg/kg); and group 4 was treated with a combination of ruxolitinib and carboplatin. The drugs were administrated by intraperitoneal injection three times per week. Tumor volume was measured every 3 days.

Bioinformatics analysis

Level 3 of The Cancer Genome Atlas (TCGA) transcriptome data on ovarian HGSC were retrieved from the Broad Institute's Genome Data Analysis Center (January 15, 2014). Data used included the transcriptome on the Affymetrix U133a platform (12). Microarray data generated by our team have been deposited in NCBI's Gene Expression Omnibus and are accessible through GEO Series accession number GSE84755 (http://www.ncbi.nlm.nih.gov/geo/query/acc.cgi?acc=GSE84755).

Statistical analysis

Statistical analyses were performed using Prism 5 software (GraphPad). Two-tailed Student *t* test was used for comparing two groups, and two-way ANOVA was used for comparing more than two groups. All results represent at least three independent replications. Wilcoxon signed rank sum test was performed to compare PBX1 expression between paired primary and recurrent tumors. Survival analyses were computed by Kaplan–Meier method and log-rank test using SPSS Statistics. Spearman rank correlation test was performed to analyze the correlation between PBX1 and target gene expression. Data are shown as mean value ± SD; $P < 0.05$ was considered statistically significant. Power calculation was performed for animal and human tissue studies with the G*Power analysis program.

Other methods can be found in the Supplementary Methods section.

Results

Comparison of PBX1-regulated and stem cell transcriptomes

We previously identified the PBX1-regulated transcriptome by comparing shRNA-mediated PBX1 silencing in OVCAR3 ovarian cancer cells with control cells without gene silencing (8). Here, we applied two methods, Ben-Porath and Gene Set Enrichment, to compare the PBX1-regulated transcriptome with the embryonic stem (ES) cell gene expression signature as well as target genes regulated by well-known ES transcription factors NANOG, OCT4, SOX2, and MYC. We found that most of the gene signatures regulated by these ES cell factors were significantly enriched in the PBX1-regulated transcriptome (Supplementary Fig. S1). Among them, the NANOG gene signature showed the highest similarity to the PBX1 transcriptome. These results indicate a molecular similarity between PBX1-regulated genes in ovarian cancer cells and genes involved in embryonic stem cells, as reflected by their coregulated genes.

Upregulation of PBX1 in recurrent, chemoresistant ovarian carcinomas

Pairs of primary (untreated) and recurrent chemoresistant tumor samples from 41 patients were analyzed using IHC to determine whether PBX1 expression levels correlated with chemotherapeutic treatment in women with HGSCs. This sample size ($n = 41$) gave us a power greater than 0.99 to accept or refute this testing hypothesis ($\alpha = 0.05$). The specificity of the anti-PBX1 antibody was validated in formalin-fixed paraffin-embedded cell blocks containing $PBX1^{high}$- and $PBX1^{low}$-expressing ovarian cancer cell lines (Supplementary Fig. S2). Immunohistochemical analysis demonstrated that PBX1 levels were significantly higher in recurrent ovarian carcinoma tissues than in matched primary carcinoma tissues (Fig. 1A, Wilcoxon signed rank sum test, $P < 0.0001$). Representative immunoreactivities of paired primary and recurrent carcinoma tissues are shown in Fig. 1B.

To determine whether PBX1 overexpression in recurrent tumors correlated with clinical outcome, we measured the PBX1 mRNA levels in effusion samples from women with ovarian HGSC. Kaplan–Meier analysis indicated that high levels of PBX1 mRNA expression (greater than the median relative expression value) in post-chemotherapy samples were associated with shorter overall survival (Fig. 1C, $P = 0.026$, log-rank test). Median overall survival was 26 months (95% CI, 21–32) in patients with PBX1 mRNA overexpression and 39 months (95% CI, 29–49) in patients without overexpression. However, PBX1 expression levels in samples acquired prior to chemotherapy were not associated with clinical outcome.

PBX1 overexpression enhances stemness and platinum resistance in ovarian cancer cells

Because chemoresistance is a hallmark of CSCs, we tested whether PBX1 expression affected responses of ovarian cancer cells to chemotherapeutic drugs routinely used in treating human cancers. *In vitro* cell viability was assessed by incubating Hey,

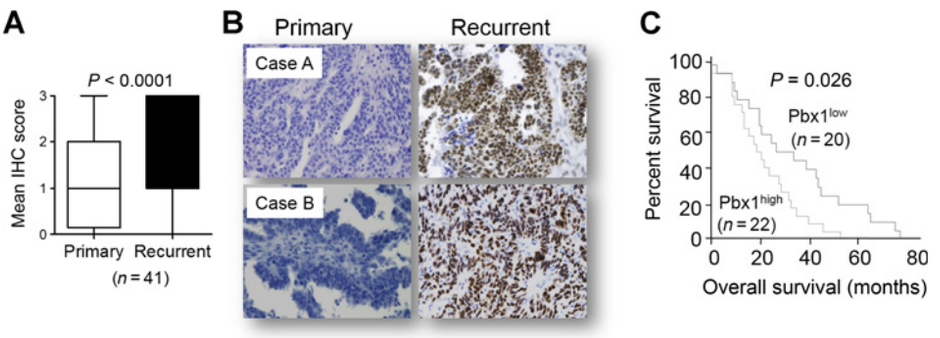

Figure 1.

High PBX1 expression in recurrent/chemoresistant ovarian carcinoma is associated with poor outcome. **A,** PBX1 immunoreactivity in a panel of matched primary and recurrent/chemoresistant ovarian carcinoma tissues ($n = 41$). PBX1 expression was evaluated independently by two investigators and was stratified into three categories based on intensity of nuclear immunoreactivity. Data represent mean ± SD, $P < 0.0001$, paired *t* test. **B,** representative examples of two pairs of matched primary and recurrent ovarian carcinomas. **C,** Kaplan–Meier analysis of 42 patients grouped by PBX1 expression levels in their ascites tumors.

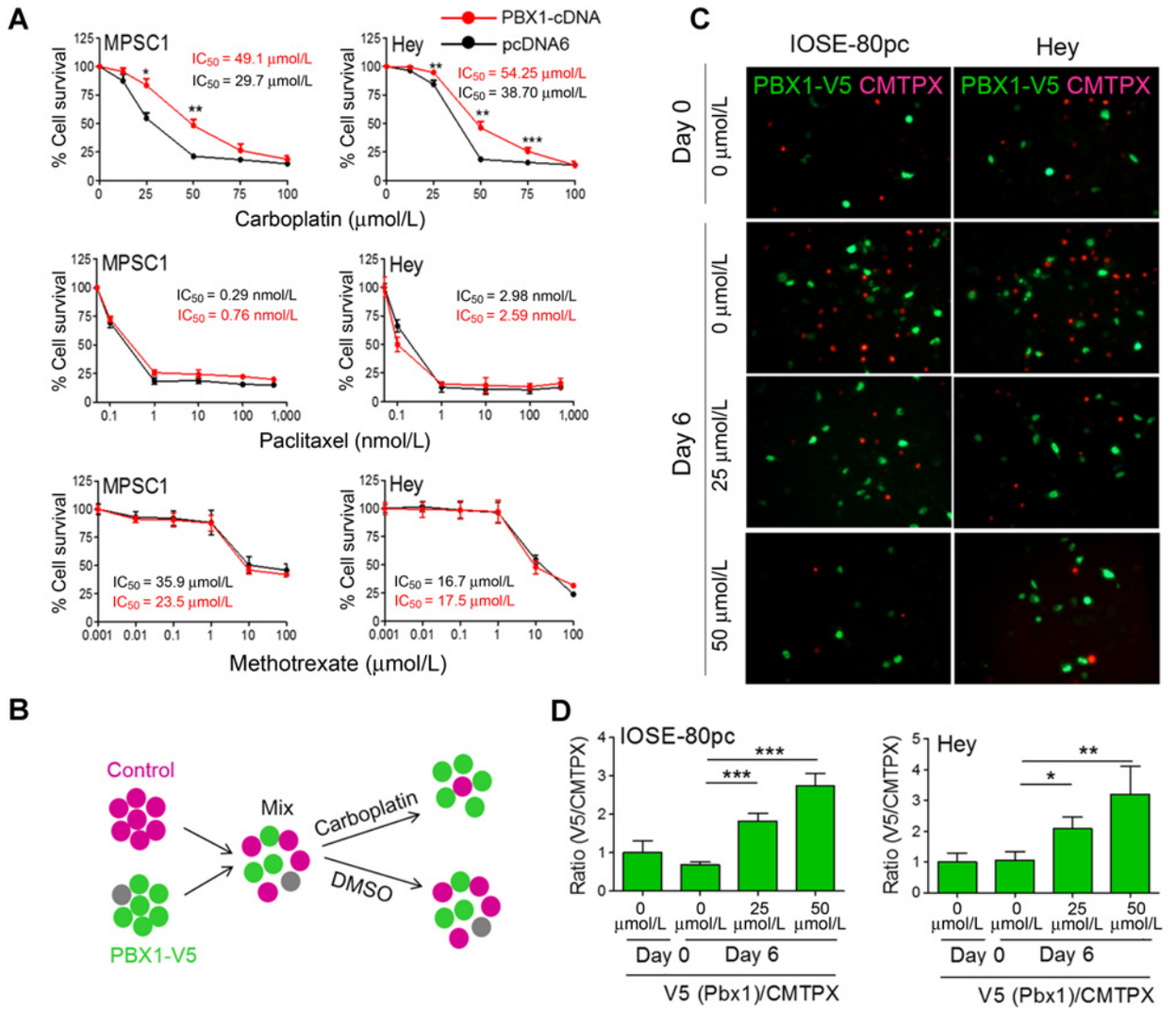

Figure 2.

PBX1 overexpression potentiates drug-resistant phenotypes. **A,** overexpression of PBX1 in Hey and MPSC1 cells enhances resistance to carboplatin but not to paclitaxel or methotrexate. Data are presented as mean ± SD. *, $P < 0.5$; **, $P < 0.01$; ***, $P < 0.005$, Student t test. **B,** schematic illustration of competition assays. An equal mixture of CMTPX-labeled (red) control cells and PBX1-V5–expressing cells were incubated in the presence or absence of carboplatin for 6 days. PBX1-V5–expressing cells were detected with an anti-V5 antibody conjugated with FITC (green). **C,** representative micrographs of cocultured PBX1-V5 and control cells treated with different concentrations of carboplatin. Experiments were performed in triplicates and were repeated three times. **D,** red or green labeled cells were counted in each of the triplicated wells, and the ratio of green/red cells was calculated. Data represent mean ± SD of three replicates. *, $P < 0.5$; **, $P < 0.01$; ***, $P < 0.005$, Student t test.

MPSC1, and IOSE-80pc cells, with or without ectopic PBX1 expression, with graded concentrations of carboplatin, paclitaxel, methotrexate, or DMSO. Ectopic PBX1 expression increased the number of cells resistant to carboplatin, but not to paclitaxel or methotrexate (Fig. 2A). Next, mixtures of PBX1-V5–transfected cells and vector-transfected control cells at equal ratios were incubated with dose-escalating carboplatin for 6 days (Fig. 2B). Control cells were labeled with cell tracker CMTPX (red), and PBX1-expressing cells were detected by anti-V5-FTIC (green). The data demonstrated that PBX1-positive cells more efficiently escaped the cytotoxic effects of carboplatin, as evidenced by an increased green to red signal ratio at day 6 in the carboplatin-treated groups (Fig. 2C and D). In contrast, the ratio of vehicle control–treated cells remained constant between day 0 and day 6, indicating no inherent difference in the growth rate between PBX1-expressing and nonexpressing cells.

To develop cellular models for functional analysis, we established platinum-resistant OVCAR3^{CR} and SKOV3^{CR} ovarian cancer cell lines. Relative to the parental cells, the resistant cells exhibited a significant increase in expression of PBX1 and its downstream target, MEOX1, and also exhibited an enhanced ability to form tumor spheroids (Supplementary Fig. S3). Furthermore, the percentage of cells in the side population and ALDH^{high} population increased in the resistant cells. Collectively, these data indicate that the platinum-resistant cells exhibit cancer stem cell phenotypes.

We also exposed IOSE-80pc and Hey cells to carboplatin (10 μmol/L) or DMSO vehicle control. One week later, $ALDH^{high}$ and $ALDH^{low}$ populations were sorted from cells exposed to each treatment (Supplementary Fig. S4A). Cells exposed to carboplatin had a higher percentage of $ALDH^{high}$ population than did DMSO-treated cells. In carboplatin-treated cells, PBX1 mRNA levels were elevated in the $ALDH^{high}$ population as compared with $ALDH^{low}$ population (Supplementary Fig. S4B). PBX1 upregulation was also observed in DMSO-treated cells, although to a much lesser degree (Supplementary Fig. S4B).

To determine whether the PBX1 signaling pathway is essential for platinum drug resistance and whether targeting PBX1 could be a potential strategy to resensitize tumor cells that are otherwise resistant to carboplatin, we treated $OVCAR3^{CR}$ and $SKOV3^{CR}$ and their parental counterparts with PBX1-specific siRNAs. The efficacy of PBX1 knockdown was assessed by both Western blot analysis (Fig. 3A, left) and qRT-PCR (Fig. 3A, right). Cell viability assay demonstrated that $OVCAR3^{CR}$ and $SKOV3^{CR}$ cells exhibited a greater response to PBX1-siRNA and platinum cotreatment than did parental cells (Fig. 3B). The IC_{50} of carboplatin was reduced approximately 3.5-fold in $OVCAR3^{CR}$ cells and approximately 2.7-fold in $SKOV3^{CR}$ cells treated with PBX1-siRNA. PBX1-siRNA did not increase carboplatin sensitivity of parental SKOV3 cells, which did not express detectable PBX1 (Fig. 3B). A moderate reduction in the IC_{50} of carboplatin was observed in the PBX1-siRNA–treated OVCAR3 cells, which expressed low levels of PBX1.

To validate the specificity of this effect, we employed a Pbx1 conditional knockout (KO) cell model using fallopian tube epithelial cells (mFTE) isolated from the $Pbx1^{fl/fl}$ mice. Treatment of mFTE cells in culture with adenovirus-Cre (Ade-Cre) induced an effective knockout of the *Pbx1* gene (Fig. 3C), but did not affect the cell growth rate (Fig. 3D). We observed that Pbx1 KO mFTE cells were more sensitive to carboplatin than were the non knocked out mFTE cells (Fig. 3E). These data lend further support to the essential role of PBX1 in the development of platinum resistance.

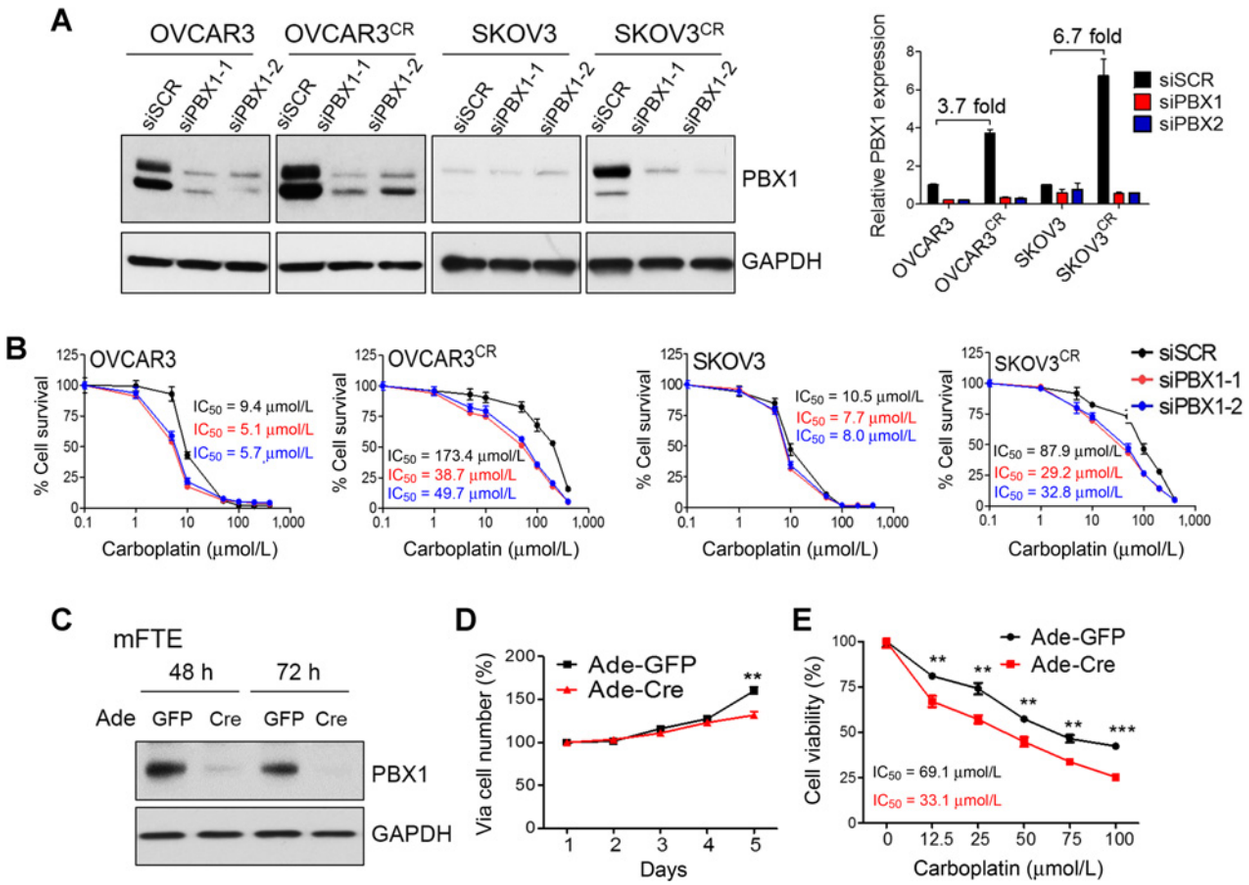

Figure 3.

PBX1 silencing enhances platinum response in ovarian cancer cells. **A,** knockdown of PBX1 by two different siRNAs in pairs of CR and parental cells determined by Western blot analysis (left) and RT-PCR (right). siSCR, scrambled control siRNA. **B,** carboplatin sensitivity assay. $OVCAR3^{CR}$ and $SKOV3^{CR}$ cells and parental OVCAR3 and SKOV3 cells were transfected with PBX1 siRNAs or scrambled control siRNA. Cell viability was measured using the CellTiter-Blue Assay Kit. **C,** Western blot analysis of Pbx1 KO cells. Immortalized fallopian tube epithelial cells (mFTE) derived from $Pbx1^{fl/fl}$ mice were exposed to Ade-Cre or Ade-GFP, and protein lysates were harvested after viral transduction. **D,** relative cell growth was measured for 5 days; data were normalized to data obtained on day 1. **E,** carboplatin sensitivity of Pbx1 KO cells. mFTE cells were transduced with Ade-Cre or Ade-GFP, and, 12 hours later, were treated with serial concentrations of carboplatin for 3 days. Cell viability is expressed as a percentage of vehicle (DMSO)-treated cells.

PBX1 regulates genes involved in stemness, tissue injury response, and drug metabolism

Using the genome-wide NimbleGen ChIP-on-chip arrays, we previously reported direct target genes of PBX1 in OVCAR3 cells (8). The high confidence promoter occupancy list (with FDR <0.05) included a total of 1,079 genes whose promoters showed significant PBX1 binding peaks (Supplementary Table S1). Among these, 5 genes belonged to the ATP binding cassette (ABC) transporter gene family. Functional Ingenuity Pathway Analysis (IPA) of PBX1 target genes demonstrated that the most significantly enriched canonical pathways were involved in glutathione redox reactions, TR/RXR activation, and JAK2 signaling (Supplementary Table S2). Genes involved in ES cell pluripotency and development, such as BMP and MEIS1, and acute-phase response factors STAT3 and JAK2 were also present. Disease and functional annotation of PBX1 target genes indicated a high degree of association with cancer and organismal injury and abnormalities (Fig. 4A). Overall, our findings suggest that PBX1 is an upstream regulator of networks that govern organismal injury, drug metabolism, and stemness in ovarian cancer cells.

To extrapolate these findings to human cancer, we analyzed expression levels of PBX1 target genes in the TCGA ovarian HGSC dataset, consisting of primary ($n = 569$) and recurrent ($n = 17$) tumors. PBX1 expression levels in recurrent tumors, but not in primary tumors, correlated with the expression of genes participating in drug metabolism and stem cell pathways. These included MEIS1 ($r = 0.63$, $P < 0.01$), RXRB ($r = 0.69$, $P < 0.005$), and NOTCH3 ($r = 0.48$, $P < 0.05$; Supplementary Fig. S5). In addition, a trend toward positive

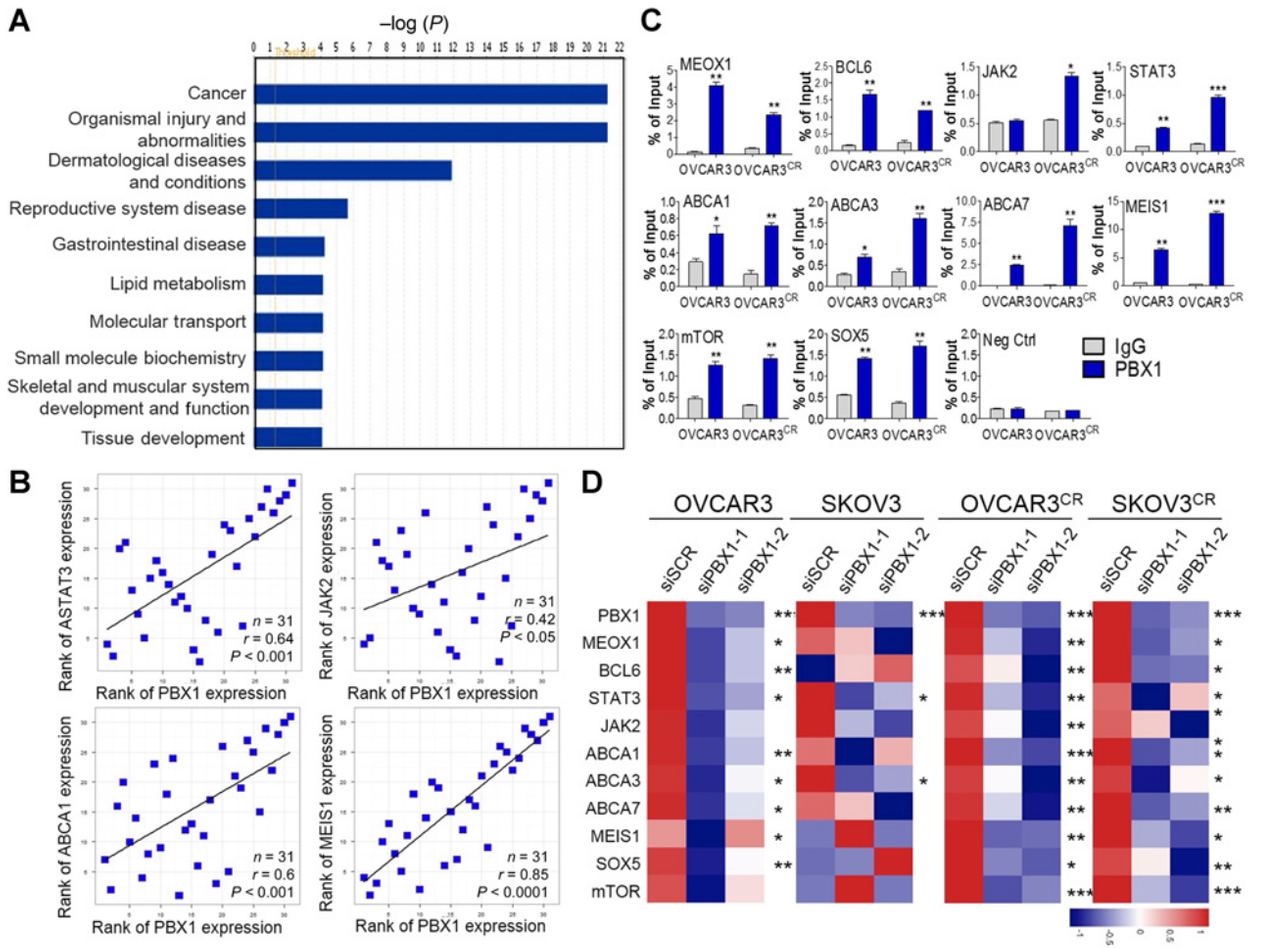

Figure 4.

PBX1 directly regulates transcription of ABC genes and stem cell factors. **A,** disease and functional annotation of PBX1 target genes analyzed by IPA. The *P* values were determined using the Fisher exact test. **B,** coexpression of PBX1 and its target genes in ascites tumors from recurrent ovarian cancer patients. Their expression levels were measured by qRT-PCR. Each point represents a ranked order of expression value for the specified genes in each sample. *r* represents Spearman rank correlation coefficient, and *P* represents two-sided Student *t* test. **C,** occupancy of target gene promoters by PBX1 was assessed by ChIP-qPCR analysis. Primers were flanking the peak of the PBX1 bound region. PCR was performed in triplicated wells, normalized to input control, and presented as mean ± SD. *, $P < 0.05$; **, $P < 0.01$; ***, $P < 0.001$; Student *t* test. **D,** color-coded heatmap representation of mRNA expression in PBX1 downstream target genes. Parental and carboplatin-resistant cells were exposed to PBX1 siRNAs or scramble control siRNAs (siSCR). Expression levels were measured by quantitative RT-PCR and normalized to siSCR-treated cells. *, $P < 0.05$; **, $P < 0.01$; ***, $P < 0.001$, one-way ANOVA.

correlation between PBX1 and STAT3, JAK2, or ABCA1 and a trend toward negative correlation between PBX1 and BMP14 or PDIA3 was observed in recurrent tumors. Since there were only a few TCGA recurrent tumors, we validated expression correlation between PBX1 and its target genes in an independent cohort consisting of 31 recurrent tumors (Fig. 4B). This sample size gave us greater than 0.90 power to determine whether the correlation was significant ($\alpha = 0.05$).

PBX1 occupancy at its target promoters was validated by ChIP-qPCR (Fig. 4C). Previously reported PBX1 target genes, MEOX1 and BCL6, were also included as positive controls. Interestingly, the degree of PBX1 binding to most target gene promoters was greater in OVCAR3^{CR} cells than in the parental cells (Fig. 4C). Following knockdown of PBX1, the expression levels of these target genes decreased in OVCAR3^{CR} and SKOV3^{CR} cells (Fig. 4D), and to a lesser degree in parental cells. In a complementary approach, ectopic PBX1 expression increased the expression of PBX1 downstream genes in ovarian cells, IOSE-80pc, MPSC1, and Hey (Supplementary Fig. S6).

The STAT3 pathway is a direct target of PBX1

Among the candidate PBX1-regulated genes, we focused on validating and characterizing STAT3 because the JAK2/STAT3 signaling pathway has been reported to confer platinum drug resistance (13, 14), and its pharmacologic inhibitors have already been developed (15, 16). First, we examined the expression of PBX1, phospho-STAT3 (pSTAT3), total STAT3 (tSTAT3), and total JAK2 (tJAK2) in parental, carboplatin-resistant, and paclitaxel-resistant tumor cells. Our results demonstrated increased STAT3 signaling activity in platinum-resistant cells as compared with parental or paclitaxel-resistant counterparts (Fig. 5A). We further used *Pbx1*$^{fl/fl}$ mFTE cells to assess STAT3 expression levels after PBX1 was knocked out. STAT3 and pSTAT3 expression levels were both decreased in cells with induced Pbx1 knockout (cells transduced by Ade-Cre)

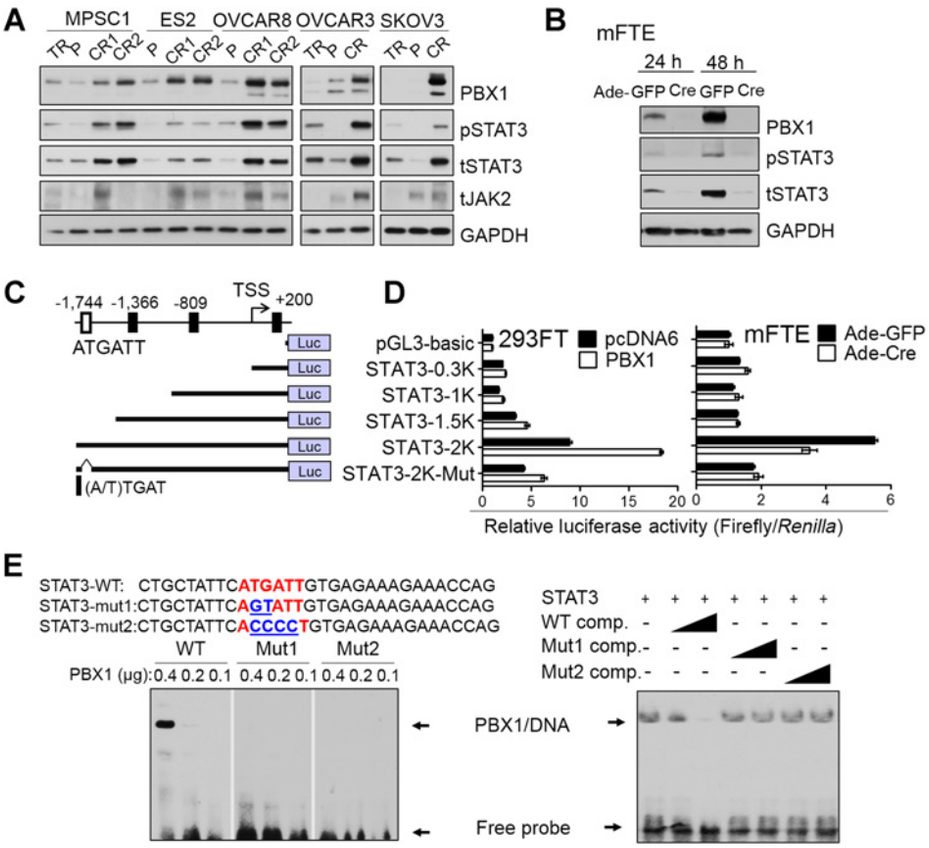

Figure 5.

PBX1 regulates the JAK2/STAT3 pathway. **A,** Western blot analysis of PBX1, phospho-STAT3 (pSTAT3), total STAT3 (tSTAT3), and total JAK2 (tJAK2) expression in taxol-resistant (TR), parental (P), and carboplatin-resistant (CR) ovarian cancer cell lines. GAPDH was used as a loading control. **B,** Western blot analysis of immortalized fallopian tube epithelial cells (mFTE) derived from *Pbx1*$^{fl/fl}$ mice. Cells were exposed to Ade-Cre or Ade-GFP. **C,** schematic presentation of *STAT3* promoter reporter construct and serial deletion mutant constructs. Rectangles, putative PBX1-binding motifs on the *STAT3* promoter. Open rectangle at −1,744 bp region represents PBX1 ChIP binding peaks identified previously (8). **D,** HEK 293FT or mFTE cells were cotransfected with the indicated firefly luciferase reporter construct, a vector encoding *Renilla* luciferase, and either PBX1-encoding vector or control vector. Relative luciferase activity was calculated by dividing firefly luciferase activity by *Renilla* luciferase activity. Data represent mean ± SD. **E,** EMSA with biotin-labeled DNA probes encompassing the PBX1 binding motif (bolded letters) and flanking sequences at the −1,744 bp region of the *STAT3* promoter. Mutant probes with 2 or 4 bp substitutions (underlined) were designed to test binding specificity. Positions of PBX1–DNA complex and free DNA probes are indicated on the gel images.

but not in cells without Pbx1 knockout (cells transduced by Ade-GFP; Fig. 5B). Because endogenous JAK2 expression was undetectable in mFTE cells, we did not perform further analysis on JAK2.

Next, we performed a luciferase promoter assay to evaluate how PBX1 regulates transcriptional activity of STAT3. A luciferase STAT3 promoter construct was generated to include sequences from −1,863 bp to +322 bp relative to the transcription start site (STAT3-2K). A series of STAT3 promoter nested deletion constructs flanking the PBX1 binding peak located at −1,744 bp region were also generated (Fig. 5C). We transfected 293FT cells with either PBX1-cDNA or empty vector along with various STAT3 promoter reporter constructs and demonstrated that ectopic expression of PBX1 in 293FT cells directly enhanced STAT3 transcriptional activity, but this was diminished when the promoter sequence from −1.5 kb to −2 kb was deleted (STAT3-1.5 K, Fig. 5C). Deletion in the −1.5 kb to −2 kb region also reduced basal activity of STAT3 transcription. In addition, a mutant construct, STAT3-2K-mut, with a 2-bp deletion in the PBX1-binding motif was created; this 2-bp deletion led to a significant reduction in both basal and PBX1-induced STAT3 transcriptional activity. The above results could be validated using the PBX1-inducible mFTE knockout model (Fig. 5D). Electrophoretic mobility shift assay (EMSA) was then performed to assess direct binding of the PBX1 protein to the STAT3 promoter sequences. A shifted band corresponding to the PBX1-bound DNA complexes was detected (Fig. 5E, left). However, the binding was abrogated by 2-bp or 4-bp substitutions in the PBX1 binding motif (Fig. 5E, left). Similarly, the binding was competitively abolished by excessive unlabeled wild-type probe, but not by the mutant probes (Fig. 5E, right).

Targeting the PBX1–STAT3 pathway reduces tumor growth in recurrent ovarian carcinomas

Ruxolitinib, an inhibitor targeting STAT3 phosphorylation and its subsequent signal activation, was used to investigate the efficacy of directly targeting STAT3 activity in platinum-resistant ovarian cancer cells with PBX1 overexpression. Approximately 1 week after inoculation with $OVCAR8^{CR}$ or $SKOV3^{CR}$ cells, mice were randomized into four groups and treated with vehicle control, ruxolitinib alone, carboplatin alone, or ruxolitinib and carboplatin combination. There were 5 mice in each group of $OVCAR8^{CR}$ and 7 in each group of $SKOV3^{CR}$. This sample size gave 0.86 power to determine whether there was a difference among four treatment groups ($\alpha = 0.05$). Mice treated with ruxolitinib and carboplatin combination exhibited significantly reduced growth rates and reduced endpoint tumor volume in both tumor models compared with mice treated with single agent or vehicle control (Fig. 6). Activities of STAT3 were assessed on the resected tumors at the study endpoint using an antibody against pSTAT3. We observed a marked reduction of the phosphorylation levels of STAT3 in the ruxolitinib-treated group and in the ruxolitinib and carboplatin combination-treated group but not in the vehicle control-treated group (Fig. 6).

Discussion

Emerging evidence has suggested that chemoresistance in human cancers can develop due to the reactivation or reprogramming of transcriptional networks critical for stem cell repopulation and tissue regeneration. We report here that PBX1 is a critical transcriptional regulator required for driving stemness and chemoresistance in ovarian cancer cells. At the tissue level, PBX1 is upregulated in recurrent as compared with the matched primary ovarian carcinomas, and its upregulation is associated with a less favorable prognosis in patients after platinum-based chemotherapy. Moreover, *in silico* analysis of genome-wide ChIP-on-chip data demonstrates that PBX1 acts as an upstream molecular hub, directly regulating genes that participate in key pathways related to stemness and drug metabolism. These findings establish a novel role of PBX1 in the development of chemoresistance, and provide a molecular basis for targeting PBX1 or its downstream effectors to overcome chemoresistance in human cancer.

PBX1 is a well-established transcription factor that regulates self-renewal of hematopoietic stem cells and participates in reprogramming lineage-committed blood cells into hematopoietic stem cells (5, 17). PBX1 also plays a key role in tissue development, as it contributes to hematopoiesis and development of pancreas, spleen, urogenital tract, and skeleton (6, 18–20). In human cancer, PBX1 was first reported as a translocated proto-oncogene in leukemia, of which the translocated gene product was shown to have an oncogenic potential (21, 22). In addition to hematopoietic malignancy, PBX1 is highly expressed in solid tumors including melanoma, prostate, ovarian, and breast cancers (23–25). In ovarian cancer, PBX1 has been identified as an effector in the NOTCH3 signaling pathway, which is known to maintain stemness and promote platinum resistance in ovarian cancer cells (10, 26). The Notch pathway has been demonstrated to regulate the PI3K/Akt pathway in stem cells (27) and to regulate ATP-binding cassette protein ABCG2 (28) that confers multidrug resistance by regulating drug efflux (28, 29).

The observation that PBX1 mediates resistance to a subset of chemotherapeutic agents such as platinum-based drugs is interesting and could be explained by at least two possibilities. First, there are more than 48 types of ATP-binding cassette proteins, each of which is characterized by unique substrate specificity (30). For example, ABCC2 and ABCC3 were previously shown to mediate platinum drug efflux, whereas ABCB4 and ABCB11 mediate efflux of other drugs such as paclitaxel (30). Our study indicates that PBX1-regulated transporters ABCA1, ABCA3, and ABCA7 are likely responsible for platinum drug efflux, thus contributing to the observed platinum resistance phenotype. Another possibility is that PBX1 mediates platinum drug resistance through its target gene, NCOA3, a nuclear steroid receptor coactivator protein that is located at a frequently amplified locus in ovarian tumors displaying innate platinum resistance (Supplementary Fig. S5; ref. 31). Collectively, our data indicate that cancer cells can potentially harness the PBX1 pathway to support cell survival, particularly under platinum chemotherapy–induced damage or stress.

Studies on hematopoiesis demonstrate that PBX1 expression maintains a viable pool of quiescent stem cells (5). In a bladder urothelial carcinoma model, chemotherapy was shown to trigger a tissue damage repair signal and stimulate cell division and repopulation of quiescent CSCs (32). Therefore, we speculate that chemotherapy in ovarian cancer may induce a comparable cell damage response and trigger PBX1 reactivation, which in turn orchestrates downstream networks essential for CSC repopulation. This hypothesis is supported by

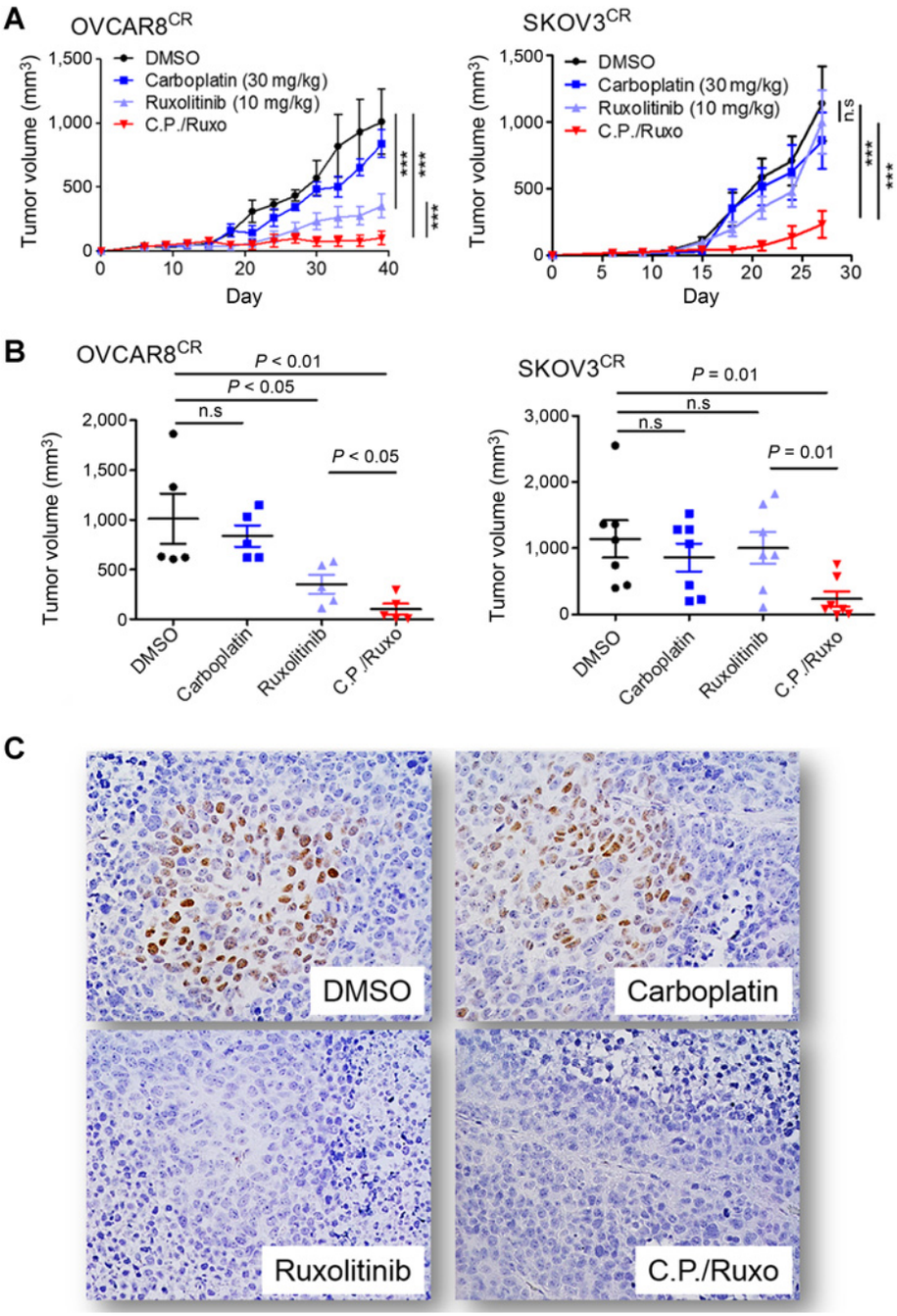

Figure 6.

Targeting Pbx1 downstream signaling pathway, JAK-STAT, effectively sensitizes tumor to carboplatin treatment. **A,** tumor growth kinetics of SKOV3^{CR} or OVCAR8^{CR} xenografts treated with DMSO, 30 mg/kg carboplatin, 10 mg/kg ruxolitinib, or 30 mg/kg carboplatin/10 mg/kg ruxolitinib combination. Treatment began 1 week after injection of 3×10^6 tumors cells; $n = 7$ per group for SKOV3^{CR}, $n = 5$ per group for OVCAR8^{CR}. ***, $P < 0.001$, one way ANOVA. **B,** endpoint tumor volume of SKOV3^{CR} or OVCAR8^{CR} xenografts treated with the indicated drug or drug combination. Student t test. **C,** representative micrographs of phospho-STAT3 immunoreactivity in SKOV3^{CR} xenografts treated with the indicated drug or drug combination.

the finding that the top PBX1-regulated pathways, including JAK2/STAT3 and IL17 signaling (CXCL3/CXCL5), are related to cytokine-mediated responses known to contribute to the remodeling of tissue microenvironment for injury repair, angiogenesis, and tumor cell migration and invasion (33–35). Our discovery that PBX1 upregulates ALDH activity is interesting because ALDH1A can be directly regulated by EZH2, a member of polycomb gene family that is overexpressed in a subset of ovarian cancers (36, 37). Because both PBX1 and EZH2 can support ovarian cancer CSCs, it would be interesting to further study a potential crosstalk between these two signaling pathways.

The association between PBX1 expression and development of drug resistance reported herein suggests that the PBX1 pathway is potentially actionable for target-based therapy. Because downregulation of PBX1 restores the chemosensitivity of carboplatin-resistant ovarian cancer cells, an approach employing a combination of PBX1 antagonists and chemotherapeutic agents may offer a better intervention to delay ovarian tumor recurrence. Another potential strategy is to target

downstream effectors of PBX1 such as JAK2/STAT3. JAK2 is a tyrosine kinase that directly phosphorylates and activates STAT3, leading to transcriptional activation of various STAT3-regulated genes that work in concert to promote tumor progression. This study demonstrates that PBX1 acts directly on the STAT3 promoter to induce STAT3 transcription, which in turn promotes platinum drug resistance. Our data further show that pharmacologic inhibition of STAT3 signaling using ruxolitinib, a clinical grade JAK2/STAT3 pathway inhibitor, in combination with carboplatin effectively suppresses *in vivo* growth of carboplatin-resistant tumors. These findings provide a strong biological rationale for testing combinations of platinum with JAK2/STAT3 inhibitors in patients who suffer from chemoresistant ovarian tumors.

Our data should not, however, be construed to suggest that STAT3 is responsible for all PBX1-mediated phenotypes. In fact, PBX1 orchestrates multiple functional networks, and additional PBX1-regulated pathway(s) that participate in CSC repopulation and chemoresistance may yet be discovered. More efforts are needed to illuminate the mechanisms through which PBX1 is reactivated or its network reprogrammed in response to challenges in the tumor environment, such as being exposed to chemotherapeutic drugs, experiencing inflammation, or encountering an alteration in host immunity. Nevertheless, our data suggest intricate functional role(s) of PBX1 in tumor cell survival during microenvironmental challenges, a research direction warranting further investigation.

Disclosure of Potential Conflicts of Interest

No potential conflicts of interest were disclosed.

Authors' Contributions

Conception and design: J.-G. Jung, I.-M. Shih, T.-L. Wang
Development of methodology: J.-G. Jung, L. Selleri, T.-L. Wang
Acquisition of data (provided animals, acquired and managed patients, provided facilities, etc.): J.-G. Jung, J.T. Park, T.H. Kim, A. Ayhan, K. Handschuh, B. Davidson, A.N. Fader, L. Selleri, T.-L. Wang
Analysis and interpretation of data (e.g., statistical analysis, biostatistics, computational analysis): J.-G. Jung, I.-M. Shih, T.H. Kim, B. Davidson, A.N. Fader, T.-L. Wang
Writing, review, and/or revision of the manuscript: J.-G. Jung, I.-M. Shih, E. Gerry, A. Ayhan, B. Davidson, A.N. Fader, L. Selleri, T.-L. Wang
Administrative, technical, or material support (i.e., reporting or organizing data, constructing databases): E. Gerry, T.H. Kim, A. Ayhan, A.N. Fader, T.-L. Wang
Study supervision: I.-M. Shih, T.-L. Wang

Acknowledgments

We wish to thank Dr. J.C. Kuan and Ms. Asli Bahadirli Talbott for assistance with Western blots and IHC. We also thank Ms. Kasthuri Nair for help in preparing this article.

Grant Support

This work was supported by the NIH grants RO1CA148826 (T.-L. Wang), R21CA187512 (T.-L. Wang), and 5RO1HD61403 (L. Selleri), Department of Defense grants W81XWH-11-2-0230 (I.-M. Shih and T.-L. Wang) and W81XWH-14-1-0221 (to T.-L. Wang), Katie Oppo Research Fund (I.-M. Shih), and The Ephraim and Wilma Shaw Roseman Foundation (A.N. Fader and I.-M. Shih).

The costs of publication of this article were defrayed in part by the payment of page charges. This article must therefore be hereby marked *advertisement* in accordance with 18 U.S.C. Section 1734 solely to indicate this fact.

Received April 5, 2016; revised July 25, 2016; accepted August 14, 2016; published OnlineFirst September 2, 2016.

References

1. Kurman RJ, Shih IM. The Dualistic model of ovarian carcinogenesis. revisited, revised, and expanded. Am J Pathol 2016;186:733–47.
2. Shipitsin M, Polyak K. The cancer stem cell hypothesis: in search of definitions, markers, and relevance. Lab Invest 2008;88:459–63.
3. Li Y, Laterra J. Cancer stem cells: distinct entities or dynamically regulated phenotypes? Cancer Res 2012;72:576–80.
4. Pohl G, Ho CL, Kurman RJ, Bristow R, Wang TL, Shih Ie M. Inactivation of the mitogen-activated protein kinase pathway as a potential target-based therapy in ovarian serous tumors with KRAS or BRAF mutations. Cancer Res 2005;65:1994–2000.
5. Ficara F, Murphy MJ, Lin M, Cleary ML. Pbx1 regulates self-renewal of long-term hematopoietic stem cells by maintaining their quiescence. Cell Stem Cell 2008;2:484–96.
6. Selleri L, Depew MJ, Jacobs Y, Chanda SK, Tsang KY, Cheah KSE, et al. Requirement for Pbx1 in skeletal patterning and programming chondrocyte proliferation and differentiation. Development 2001;128: 3543–57.
7. Kelm JM, Timmins NE, Brown CJ, Fussenegger M, Nielsen LK. Method for generation of homogeneous multicellular tumor spheroids applicable to a wide variety of cell types. Biotechnol Bioeng 2003;83:173–80.
8. Thiaville MM, Stoeck A, Chen L, Wu RC, Magnani L, Oidtman J, et al. Identification of PBX1 target genes in cancer cells by global mapping of PBX1 binding sites. PLoS One 2012;7:e36054.
9. Jung JG, Stoeck A, Guan B, Wu RC, Zhu H, Blackshaw S, et al. Notch3 interactome analysis identified WWP2 as a negative regulator of Notch3 signaling in ovarian cancer. PLoS Genet 2014;10:e1004751.
10. Park JT, Shih Ie M, Wang TL. Identification of pbx1, a potential oncogene, as a notch3 target gene in ovarian cancer. Cancer Res 2008;68:8852–60.
11. Chen X, Thiaville MM, Chen L, Stoeck A, Xuan J, Gao M, et al. Defining NOTCH3 target genes in ovarian cancer. Cancer Res 2012; 72:2294–303.
12. Broad Institute TCGA Genome Data Analysis Center. Analysis-ready standardized TCGA data from Broad GDAC Firehose stddata_2014_01_15 run. Boston, MA: Broad Institute of MIT and Harvard; 2014.
13. Costantino L, Barlocco D. STAT 3 as a target for cancer drug discovery. Curr Med Chem 2008;15:834–43.
14. Bourguignon LY, Peyrollier K, Xia W, Gilad E. Hyaluronan-CD44 interaction activates stem cell marker Nanog, Stat-3-mediated MDR1 gene expression, and ankyrin-regulated multidrug efflux in breast and ovarian tumor cells. J Biol Chem 2008;283:17635–51.
15. Hedvat M, Huszar D, Herrmann A, Gozgit JM, Schroeder A, Sheehy A, et al. The JAK2 inhibitor AZD1480 potently blocks Stat3 signaling and oncogenesis in solid tumors. Cancer Cell 2009;16:487–97.
16. Eghtedar A, Verstovsek S, Estrov Z, Burger J, Cortes J, Bivins C, et al. Phase 2 study of the JAK kinase inhibitor ruxolitinib in patients with refractory leukemias, including postmyeloproliferative neoplasm acute myeloid leukemia. Blood 2012;119:4614–8.
17. Riddell J, Gazit R, Garrison BS, Guo G, Saadatpour A, Mandal PK, et al. Reprogramming committed murine blood cells to induced hematopoietic stem cells with defined factors. Cell 2014;157:549–64.
18. Kim SK, Selleri L, Lee JS, Zhang AY, Gu X, Jacobs Y, et al. Pbx1 inactivation disrupts pancreas development and in Ipf1-deficient mice promotes diabetes mellitus. Nat Genet 2002;30:430.
19. Brendolan A, Ferretti E, Salsi V, Moses K, Quaggin S, Blasi F, et al. A Pbx1-dependent genetic and transcriptional network regulates spleen ontogeny. Development 2005;132:3113–26.
20. Schnabel CA, Godin RE, Cleary ML. Pbx1 regulates nephrogenesis and ureteric branching in the developing kidney. Dev Biol 2003;254:262.
21. Nourse J, Mellentin JD, Galili N, Wilkinson J, Stanbridge E, Smith SD, et al. Chromosomal translocation t(1;19) results in synthesis of a homeobox fusion mRNA that codes for a potential chimeric transcription factor. Cell 1990;60:535–45.

22. Kamps MP, Look AT, Baltimore D. The human t(1;19) translocation in pre-B ALL produces multiple nuclear E2A-Pbx1 fusion proteins with differing transforming potentials. Genes Dev 1991;5:358–68.
23. Shiraishi K, Yamasaki K, Nanba D, Inoue H, Hanakawa Y, Shirakata Y, et al. Pre-B-cell leukemia transcription factor 1 is a major target of promyelocytic leukemia zinc-finger-mediated melanoma cell growth suppression. Oncogene 2007;26:339–48.
24. Yeh HY, Cheng SW, Lin YC, Yeh CY, Lin SF, Soo VW. Identifying significant genetic regulatory networks in the prostate cancer from microarray data based on transcription factor analysis and conditional independency. BMC Med Genomics 2009;2:70–89.
25. Magnani L, Stoeck A, Zhang X, Lanczky A, Mirabella AC, Wang TL, et al. Genome-wide reprogramming of the chromatin landscape underlies endocrine therapy resistance in breast cancer. Proc Natl Acad Sci U S A 2013;110: E1490–9.
26. Park JT, Chen X, Trope CG, Davidson B, Shih Ie M, Wang TL. Notch3 overexpression is related to the recurrence of ovarian cancer and confers resistance to Carboplatin. Am J Pathol 2010;177:1087–94.
27. Wang J, Wakeman TP, Lathia JD, Hjelmeland AB, Wang XF, White RR, et al. Notch promotes radioresistance of glioma stem cells. Stem Cells 2010; 28:17–28.
28. Bhattacharya S, Das A, Mallya K, Ahmad I. Maintenance of retinal stem cells by Abcg2 is regulated by notch signaling. J Cell Sci 2007;120:2652–62.
29. Dean M, Fojo T, Bates S. Tumour stem cells and drug resistance. Nat Rev Cancer 2005;5:275–84.
30. Gottesman MM, Fojo T, Bates SE. Multidrug resistance in cancer: role of ATP-dependent transporters. Nat Rev Cancer 2002;2:48–58.
31. Etemadmoghadam D, deFazio A, Beroukhim R, Mermel C, George J, Getz G, et al. Integrated genome-wide DNA copy number and expression analysis identifies distinct mechanisms of primary chemoresistance in ovarian carcinomas. Clin Cancer Res 2009;15:1417–27.
32. Kurtova AV, Xiao J, Mo Q, Pazhanisamy S, Krasnow R, Lerner SP, et al. Blocking PGE2-induced tumour repopulation abrogates bladder cancer chemoresistance. Nature 2015;517:209–13.
33. Korkaya H, Liu S, Wicha MS. Breast cancer stem cells, cytokine networks, and the tumor microenvironment. J Clin Invest 2011;121:3804–9.
34. Chung EY, Liu J, Homma Y, Zhang Y, Brendolan A, Saggese M, et al. Interleukin-10 expression in macrophages during phagocytosis of apoptotic cells is mediated by homeodomain proteins Pbx1 and Prep-1. Immunity 2007;27:952–64.
35. Yu H, Lee H, Herrmann A, Buettner R, Jove R. Revisiting STAT3 signalling in cancer: new and unexpected biological functions. Nat Rev Cancer 2014;14:736–46.
36. Li H, Bitler BG, Vathipadiekal V, Maradeo ME, Slifker M, Creasy CL, et al. ALDH1A1 is a novel EZH2 target gene in epithelial ovarian cancer identified by genome-wide approaches. Cancer Prev Res 2012;5: 484–91.
37. Landen CN Jr, Goodman B, Katre AA, Steg AD, Nick AM, Stone RL, et al. Targeting aldehyde dehydrogenase cancer stem cells in ovarian cancer. Mol Cancer Ther 2010;9:3186–99.